Bioorganic & Medicinal Chemistry xxx (2016) xxx–xxx

Contents lists available at ScienceDirect

Bioorganic & Medicinal Chemistry

journal homepage: www.elsevier.com/locate/bmc

Synthesis, molecular modeling and SAR study of novel pyrazolo[5,1-*f*][1,6]naphthyridines as CB_2 receptor antagonists/inverse agonists

Antonio Dore [a], Battistina Asproni [a,*], Alessia Scampuddu [a], Stefania Gessi [b,*], Gabriele Murineddu [a], Elena Cichero [c], Paola Fossa [c], Stefania Merighi [b], Serena Bencivenni [b], Gérard A. Pinna [a]

[a] Dipartimento di Chimica e Farmacia, Università degli Studi di Sassari, Via F. Muroni 23/a, 07100 Sassari, Italy
[b] Dipartimento di Scienze Mediche, Sezione di Farmacologia, Università di Ferrara, Via Fossato di Mortara, 17-19, 44121 Ferrara, Italy
[c] Dipartimento di Farmacia, Università di Genova, Viale Benedetto XV n. 3, 16132 Genova, Italy

ARTICLE INFO

Article history:
Received 27 May 2016
Revised 5 August 2016
Accepted 27 August 2016
Available online xxxx

Keywords:
Pyrazolo[5,1-*f*][1,6]naphthyridine
Cannabinoid receptors
CB_2 antagonism/inverse agonism
Docking studies

ABSTRACT

Pyrazolo[5,1-*f*][1,6]naphthyridine-carboxamide derivatives were synthesized and evaluated for the affinity at CB_1 and CB_2 receptors. Based on the AgOTf and proline-cocatalyzed multicomponent methodology, the ethyl 5-(*p*-tolyl)pyrazolo[5,1-*f*][1,6]naphthyridine-2-carboxylate (**12**) and ethyl 5-(2,4-dichlorophenyl)pyrazolo[5,1-*f*][1,6]naphthyridine-2-carboxylate (**13**) intermediates were synthesized from the appropriate *o*-alkynylaldehydes, *p*-toluenesulfonyl hydrazide and ethyl pyruvate. Most of the novel compounds feature a *p*-tolyl (**8a–i**) or a 2,4-dichlorophenyl (**8j**) motif at the C_5-position of the tricyclic pyrazolo[5,1-*f*][1,6]naphthyridine scaffold. Structural variation on the carboxamide moiety at the C_2-position includes basic monocyclic, terpenoid and adamantine-based amines. Among these derivatives, compound **8h** (*N*-adamant-1-yl-5-(*p*-tolyl)pyrazolo[5,1-*f*][1,6]naphthyridine-2-carboxamide) exhibited the highest CB_2 receptor affinity (K_i = 33 nM) and a high degree of selectivity (K_iCB_1/K_iCB_2 = 173:1), whereas a similar trend in the near nM range was seen for the bornyl analogue (compound **8f**, K_i = 53 nM) and the myrtanyl derivative **8j** (K_i = 67 nM). Effects of **8h**, **8f** and **8j** on forskolin-stimulated cAMP levels were determined, showing antagonist/inverse agonist properties for such compounds. Docking studies conducted for these derivatives and the reference antagonist/inverse agonist compound **4** (SR144528) disclosed the specific pattern of interactions probably related to the pyrazolo[5,1-*f*][1,6]naphthyridine scaffold as CB_2 inverse agonists.

1. Introduction

The endocannabinoid system indicates a whole signaling system that comprises cannabinoid receptors, endogenous ligands exemplified by *N*-arachidonoylethanolamine (AEA, anandamide) **1** and 2-arachidonoylglycerol (2-AG) **2** (Fig. 1) and enzymes for ligand biosynthesis and inactivation.[1,2] This signaling system plays a crucial role in numerous physiological and pathological functions and it is involved in maintaining the physiological steady state and homeostasis.[3]

There are two subtypes of cannabinoid receptors discovered so far, the cannabinoid type 1 receptor (CB_1R) and the cannabinoid type 2 receptor (CB_2R),[4] which belong to the rhodopsin-like family of G-protein-coupled receptors (GPCRs).[5] Even before the endogenous ligands were known, CBRs have been described to be activated by terpenoid plant constituents, e.g., by Δ^9-tetrahydrocannabinol (Δ^9-THC) **3**, the major psychoactive component of *Cannabis sativa*.[6]

The CB_1Rs are abundantly expressed in the central nervous system (CNS) and are responsible for the psychotropic effects observed with nonselective cannabinoid ligands.[7–10] The CB_2Rs were initially identified as a peripherally restricted receptors predominantly expressed in cells of the human immune system,[11–13] and therefore playing an important role in mediating the immune-modulatory function.[14] Subsequent data, however, have also demonstrated the presence of CB_2Rs in brain, albeit to a much lesser extent,[15] myocardium, cardiomyoblasts and endothelian cells of various origins.[16]

Recent studies have demonstrated that CB_2Rs are involved in numerous diseases.[17] Several selective CB_2R agonists exhibited analgesic activity in preclinical models of acute, inflammatory and neuropathic pain.[18–21] Furthermore, CB_2R agonists have been evaluated for efficacy in ameliorating disease progression in in vivo models of multiple sclerosis,[22] Alzheimer's disease,[23] as well as amyotrophic lateral sclerosis.[24] Recent findings highlight

* Corresponding authors. Tel.: +39 079 228749 (B.A.), +39 0532 455332 (S.G.).
E-mail addresses: asproni@uniss.it (B. Asproni), gss@unife.it (S. Gessi).

http://dx.doi.org/10.1016/j.bmc.2016.08.055
0968-0896/

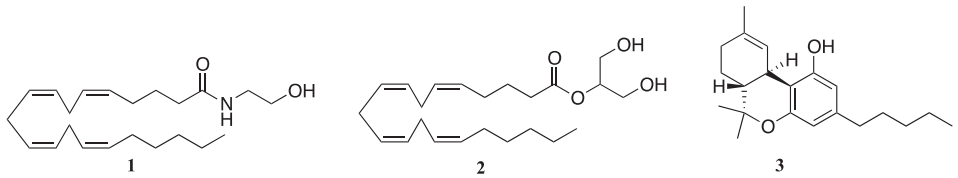

1
AEA (anandamide)
K_i CB_1 = 89 nM
K_i CB_2 = 371 nM

2
2-AG
K_i CB_1 = 472 nM
K_i CB_2 = 1400 nM

3
Δ^9-THC
K_i CB_1 = 41 nM
K_i CB_2 = 36 nM

Figure 1. The major endogenous ligands and Δ^9-THC for cannabinoid receptors.

the emerging interest in the development of CB_2R inverse agonists effective for the control of immune cell mobility in arthritis and autoimmune encephalomyelitis[25] and for the treatment of osteoporosis via the inhibition of osteoclast differentiation.[26] CB_2R neutral antagonist ligands have been recently described.[27] Such compounds could be useful to ascertain more in detail the role of CB_2 receptor in physiopathological conditions.

Because of the therapeutic potential of CB_2 ligands, there has been an increasing interest in identifying a huge diversity of chemical scaffolds for CB_2 interaction. Within this frame, hundreds of bioactive CB_2R ligands have been discovered[17,18] and among them, pyrazole derivatives **4** (SR144528)[28] and **5**[29] emerged as important prototypical CB_2 selective ligands (Fig. 2). Compound **4** from Sanofi was identified as the first potent and selective antagonist/inverse agonist of the CB_2R. Molecular modeling studies carried out on **4**[30] highlighted the importance of the C_3 carboxamide moiety together with N_1-methylbenzyl and C_5-chloromethylphenyl substituents for CB_2R affinity. A fenchyl group as carboxamide substituent is important for productive CB_2R interaction. Pyrazole derivative **5** from our lab is a dihydroindenopyrazol-based compound and belongs to one of the first tricycles to be described for CBR affinity. Structure activity-relationship (SAR) studies performed on compound **5** revealed that the flattening of the plane of the tricyclic core was a determining factor in its very high CB_2-affinity, exceptional selectivity over CB_1R, and CB_2 agonist activity in vitro. Tricyclic derivatives **6**[31] and **7**[32] feature, respectively, a dihydrothienocyclopentapyrazole and benzofuropyrazole scaffolds. Interestingly, both compounds kept the affinity for CB_2R in the nM range and were endowed with a good selectivity over CB_1R, even if it was lower than that elicited by compound **4** and **5**.

Pursuing our interest in expanding SAR studies on CB_2R, we thought that the planar pyrazolo[5,1-*f*][1,6]naphthyridine **8** (Fig. 3) could be an attractive scaffold for designing novel CB_2 ligands. Looking at the structure of compounds **4**–**7**, we postulated that the introduction of the carboxamide moiety and the pendant N_1-benzyl substituent into the tricyclic core **8** might provide novel CB_2 agonist, antagonist, inverse agonist ligands with potential therapeutic value. Thus novel compounds that varied the carboxamide moiety and the phenyl substitution were designed (Fig. 3 and Table 1). In this paper we report the synthesis of compounds **8a**–**k** together with preliminary aspects of their receptor affinity, selectivity, biological activities and molecular modeling studies. These data are accompanied by a thorough in silico evaluation of the pharmacokinetic and toxicity properties of the most potent derivatives here disclosed, with the aim at gaining preliminary information concerning their potentially drug-like profile.

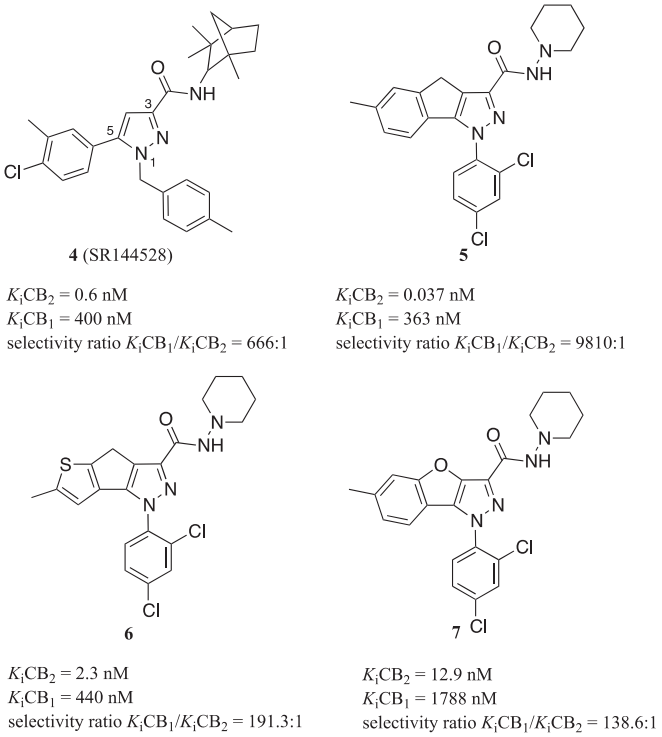

4 (SR144528)
K_iCB_2 = 0.6 nM
K_iCB_1 = 400 nM
selectivity ratio K_iCB_1/K_iCB_2 = 666:1

5
K_iCB_2 = 0.037 nM
K_iCB_1 = 363 nM
selectivity ratio K_iCB_1/K_iCB_2 = 9810:1

6
K_iCB_2 = 2.3 nM
K_iCB_1 = 440 nM
selectivity ratio K_iCB_1/K_iCB_2 = 191.3:1

7
K_iCB_2 = 12.9 nM
K_iCB_1 = 1788 nM
selectivity ratio K_iCB_1/K_iCB_2 = 138.6:1

Figure 2. Chemical structures of CB_2 selective ligands.

2. Chemistry

The synthetic route to the title compounds **8a**–**k** is outlined in Scheme 1. Based on the AgOTf and proline-cocatalyzed multicomponent methodology,[33] the key intermediates ethyl 5-(*p*-tolyl) pyrazolo[5,1-*f*][1,6]naphthyridine-2-carboxylate (**12**) and ethyl 5-(2,4-dichlorophenyl)pyrazolo[5,1-*f*][1,6]naphthyridine-2-carboxylate (**13**) were synthesized from the appropriate *o*-alkynylaldehydes, *p*-toluenesulfonyl hydrazide (PTSH) and ethyl pyruvate.

Thus, 2-bromonicotinaldehyde **9** was allowed to react with appropriate alkynes under the conventional Sonogashira conditions to give the corresponding *o*-alkynylaldehydes **10**,**11** in good yields. Compounds **10**,**11** were condensed in situ with PTSH in the presence of AgOTf (10 mol%), DL-proline (10 mol%), to give the corresponding hydrazones **10′**,**11′** (not isolated), which were converted into the desired tricyclic pyrazoles **12**,**13** by sequential treatment with ethyl pyruvate, heating the reaction mixture by microwave irradiation to 50–60 °C, and with Na_2CO_3 at room temperature. The starting *o*-alkynylaldehyde **10**, bearing the electron-donating $-CH_3$ group in *para* position to the triple bond of the phenyl ring was found to be suitable to trigger the heterocyclization reaction,[33] and provided the desired pyrazole ester **12** in 64% yield. Also the *o*-alkynylaldehyde **11**, featuring the electron-withdrawing 2,4-dichlorophenyl group proved to be favorable for the reaction, even if the corresponding pyrazole ester **13** was obtained in 49% yield. The hydrolysis of **12**,**13** with NaOH in THF afforded the acid precursors **14**,**15** in almost quantitative yield. Finally, the acids **14** and **15** were treated with pivaloyl chloride

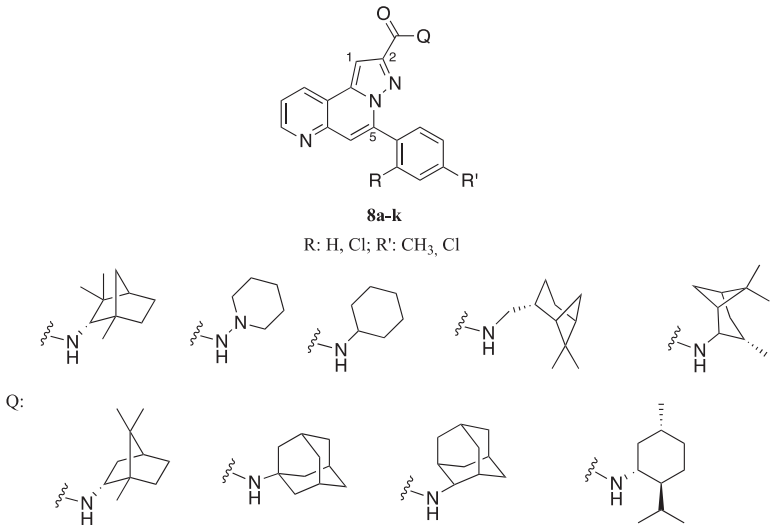

Figure 3. Novel 5-aryl-pyrazolo[5,1-*f*][1,6]naphthyridine-2-carboxamides **8a–k**.

and then with the appropriate amine to provide the desired carboxamides **8a–k**
(23–76% yield).

3. Results and discussion

3.1. Cannabinoid receptor binding studies

The CB_1 and CB_2 receptor binding affinities of the novel pyrazolo[5,1-*f*][1,6]naphthyridine derivatives **8a–k** were evaluated by radioligand binding assays performed by using transfected human CB_1 and CB_2 Chinese hamster ovary (CHO) cells. [^{3}H]CP-55,940 was employed as radiolabeled ligand. The experimental data (IC_{50} values) were converted into K_i values.[34] The receptor affinities are shown in Table 1. For comparison, the K_i value of the mixed CB_1/CB_2 ligand WIN 55,212-2 is reported. Our initial results showed that the introduction of a fenchyl group at the C_2 carboxamide portion in combination with a *p*-tolyl group at the C_5 position of the pyrazolo[5,1-*f*][1,6]naphthyridine scaffold gave compound **8a** endowed with negligeable affinity for CB_1R (K_iCB_1 = 2200 nM) and low affinity for CB_2R (K_iCB_2 = 800 nM). Further, replacement of the *N*-fenchyl moiety of **8a** with *N*-piperidinyl (**8b**) and *N*-cyclohesyl (**8c**) tail-pieces resulted in total loss of affinity for both CB_1 and CB_2Rs. To further explore whether improvements in CBR-affinity might be obtained by modifying the C_2-carboxamide side group, we next synthesized a small library of four monoterpene derivatives (**8d–g**) and two adamantine compounds (**8h,i**). Interestingly, all these compounds exhibited improved CB_2R affinity, almost total loss of affinity for CB_1R, and improved CB_1 to CB_2 selectivity than did **8a**. Among the monoterpene series, compound **8f**, featuring a bornyl group, emerged for its high CB_2R affinity (**8f**: K_i = 53 nM vs **8a**: K_i = 800 nM) and CB_1 to CB_2 selectivity (**8f**: K_iCB_1/K_iCB_2 = 132:1 vs **8a**: K_iCB_1/K_iCB_2 = 2.7:1). Concerning the adamantine derivatives, compound **8h** featuring a 1-adamantyl group, exhibited the higher CB_2R affinity and CB_1 to CB_2 selectivity among all the synthesized compounds (**8h**: K_i = 33 nM, K_iCB_1/K_iCB_2 = 173:1). Finally, compound **8j**, derived from compound **8d** by replacing the *p*-tolyl group at the C_5-position with a dichlorophenyl group, exhibited improved CB_2R affinity (**8j**: K_i = 67 nM vs **8d**: K_i = 120 nM) and selectivity (**8j**: K_iCB_1/K_iCB_2 = >149:1 vs **8d**: K_iCB_1/K_iCB_2 = 83:1), highlighting the versatility of the planar pyrazolo[5,1-*f*][1,6]naphthyridine scaffold to determine CB_2R affinity and selectivity.

3.2. Intrinsic activity by in vitro assay

The compounds **8f**, **8h**, and **8j** characterized by the best affinity and selectivity toward CB_2 receptors were investigated to evaluate their activity as agonists or antagonists on CB_2 receptors in functional assays. In particular their ability to affect forskolin-stimulated cAMP levels in human CB_2 CHO cells has been evaluated and compared to WIN 55,212-2. As shown in Figure 4, the reference agonist WIN 55,212-2 (0.1 μM) was able to inhibit forskolin-stimulated cAMP levels of 52% and all the compounds under examination were able to antagonize this effect in the range of concentration 0.1–10 μM, with the **8h** being the most potent compound, according to binding data.

To evaluate in more detail the potency of compounds to antagonize cAMP inhibition induced by WIN 55,212-2 a Schild analysis was performed. Compound **8h** shifted the concentration–response curve of WIN 55,212-2 to the right, in a concentration-dependent manner (Fig. 5A). A Schild plot of the data gave a line with a slope near unity (1.05 + 0.06) and K_B value of 316 + 47 nM (Fig. 5B). Analogously, compounds **8f** and **8j** present a K_B value of 505 ± 61 and 650 ± 74 nM, respectively. Therefore, the compounds investigated appear weaker in the functional assay respect to the binding test. However, these shifts have been repeatedly reported in the literature for different GPCRs and also for CB_2 receptors.[35] Moreover, the values of CB_2 affinity in binding assay and functional tests have not to be necessarily identical. What is interesting to note is that a good correlation between receptor affinity (K_i) and efficacy (K_B) was observed because the order of potency between the affinity and potency values is the same. Nevertheless, we could hypothesize that the discrepancy concerning the affinity values found between binding and functional test derive from the different experimental conditions between these assays, e.g., ionic strength of the buffer, time and temperature of the incubations.

Furthermore **8f** and **8j** ligands were able to increase forskolin-stimulated cAMP production at 1–10 μM, while **8h** compound started its significant effect at 0.1 μM (Fig. 6). These results characterize the compounds **8f**, **8h**, and **8j** as antagonists/inverse agonists at CB_2R. Accordingly, it has been shown that also the commercially available CB_2 receptor ligand AM630 behaves as neutral antagonist, or agonist, or inverse agonist depending on the bioassay type or cell line.[36] This may be explained based on the two-state model theory of GPCRs in which ligands depending on their affinity for

Table 1
Structures and binding data[a] for compounds **8a–k** and WIN 55,212-2

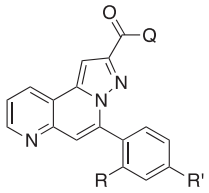

8a-k

Compd	R	R′	Q	Receptor affinity (nM)		CB_2 selectivity
				K_iCB_1	K_iCB_2	K_iCB_1/K_iCB_2
8a	H	CH_3	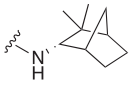	2200 ± 190	800 ± 84	2.7
8b	H	CH_3	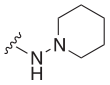	>10,000	>1000	-
8c	H	CH_3	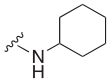	>10,000	2133 ± 230	>4.7
8d	H	CH_3	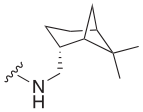	>10,000	120 ± 15	>83
8e	H	CH_3	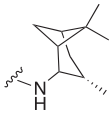	>10,000	240 ± 28	>42
8f	H	CH_3	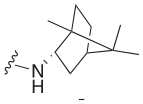	7000 ± 680	53 ± 7	132
8g	H	CH_3	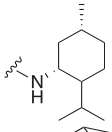	3300 ± 270	280 ± 30	12
8h	H	CH_3	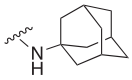	5700 ± 550	33 ± 2	173
8i	H	CH_3	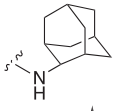	>10,000	133 ± 15	>75
8j	Cl	Cl	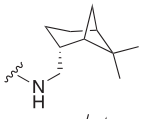	>10,000	67 ± 8	>149
8k	Cl	Cl	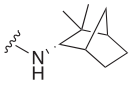	ND[b]	ND	
WIN 55,212-2				13 ± 2	2.5 ± 0.3	5.2

[a] Affinity of compounds to CB_1R and CB_2R was assayed using transfected human CB_1 and CB_2 CHO cells and [^{3}H]CP-55,940 as radiolabeled ligand. K_i values are the mean ± SEM of at least three independent experiments run in triplicate.
[b] ND, not determined.

the receptor may shift it from an inactive to an active state, when they are agonists, or vice versa, in the case of inverse agonists. In addition, compounds not producing any shift in active/inactive receptor ratio are defined neutral antagonists.[37] Therefore, our compounds appear as inverse agonists in the absence of WIN 55,212-2 while as antagonists in its presence.

3.3. Molecular modeling studies

In this work, in order to rationalize the pharmacological results concerning the most promising derivatives **8f**, **8h** and **8j** and to refine our computational model, which could guide further synthetic efforts, docking studies on **8f**, **8h** and **8j** were also performed (see Supplementary data, Table 1). In this way, we disclosed the

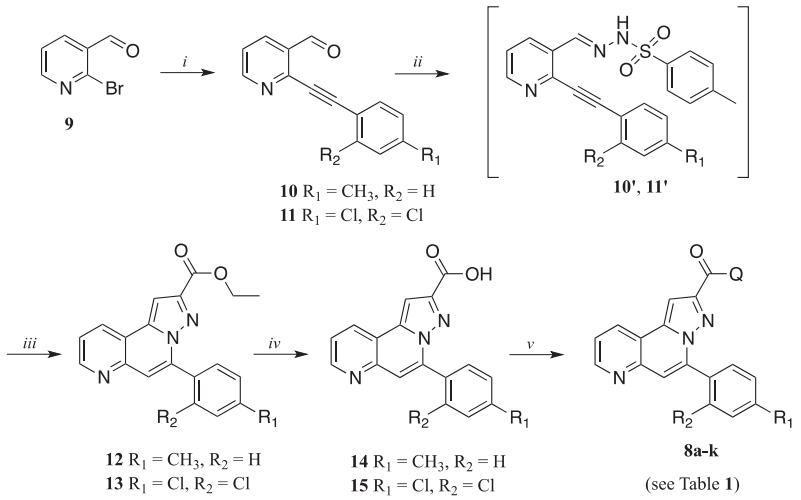

Scheme 1. Reagent and conditions: (i) *p*-tolylacetylene (for **10**) or 2,4-dichlorophenylacetylene (for **11**), $Pd(PPh_3)_2Cl_2$, CuI, Et_3N, dry DMF, MW 60 °C, 20 min; (ii) PTSH, AgOTf, DL-proline, dry EtOH, rt 10 min. (iii) (a) Ethyl pyruvate, MW 60 °C, 3.5 h; (b) Na_2CO_3, rt 12 h; (iv) NaOH, THF, 40 °C, 3 h; (v) (a) pivaloyl chloride, Et_3N, dry CH_2Cl_2, 0 °C to rt, 2 h; (b) amine, CH_2Cl_2, Et_3N, 0 °C to rt, 2.5 h.

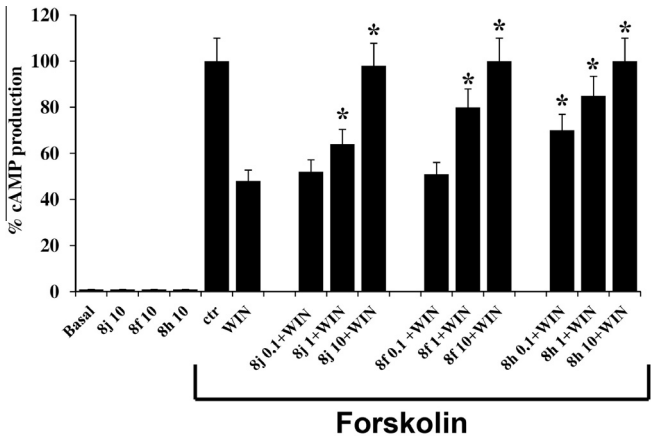

Figure 4. Inhibition of forskolin-stimulated cAMP levels (100%) by WIN 55,212-2 (0.1 μM) and antagonism by **8j**, **8f**, and **8h** (0.1–10 μM) in hCB_2CHO cells. Forskolin (10 μM) effect was set to 100%. The effect of compounds alone **8j**, **8f**, and **8h** (10 μM) is shown. Values are the mean ± SEM of four independent experiments ($N = 4$). $^*P < 0.05$, compared with WIN 55,212-2; analysis was by ANOVA followed by Dunnett's test.

specific pattern of interactions probably related to the pyrazolo [5,1-*f*][1,6]naphthyridine scaffold as CB_2 inverse agonists.

This kind of approach relied on a ligand-based homology model of the human CB_2 receptor we previously built around the chemical scaffold of the potent ligand **4** (SR144528), revealing a pool of key residues involved in the antagonist binding.[38] Notably, our results were in agreement with those discussed by Montero and coworkers about the putative antagonist binding site of the hCB_2 receptor.[39]

Thus, according to our calculations and also in agreement with recent data reported in literature, the interactions of the inverse agonists with the receptor included H-bonds at least with S165 for weaker compounds, or both the T114 and S165 residues for the most potent derivatives.[35]

In particular, the SR144528 4-chloro-3-methyl-phenyl and the benzyl group were projected toward two hydrophobic pockets including L195, Y190, W194 and I110, L169, respectively. On the other hand, the fenchyl portion was surrounded by L160, V164, F197 and F202.

These findings allowed us to highlight the key role played by a bulky group in proximity of the third hydrophobic pocket in terms of selectivity issue. Indeed, the CB_2 V164 corresponds to an isoleucine residue at the CB_1 protein, determining specific steric requirements for the binding to CB_1 and, therefore, for CB_2 selectivity. Notably, all these data are also supported by the computational studies we performed within a series of tricyclic pyrazole carboxamides as CB_2 inverse agonists.[40] According to our calculations, in this study, compounds **8f**, **8h** and **8j** share quite a similar behavior if compared with that of SR144528, displaying an overall pattern of interactions including the required H-bonds and a

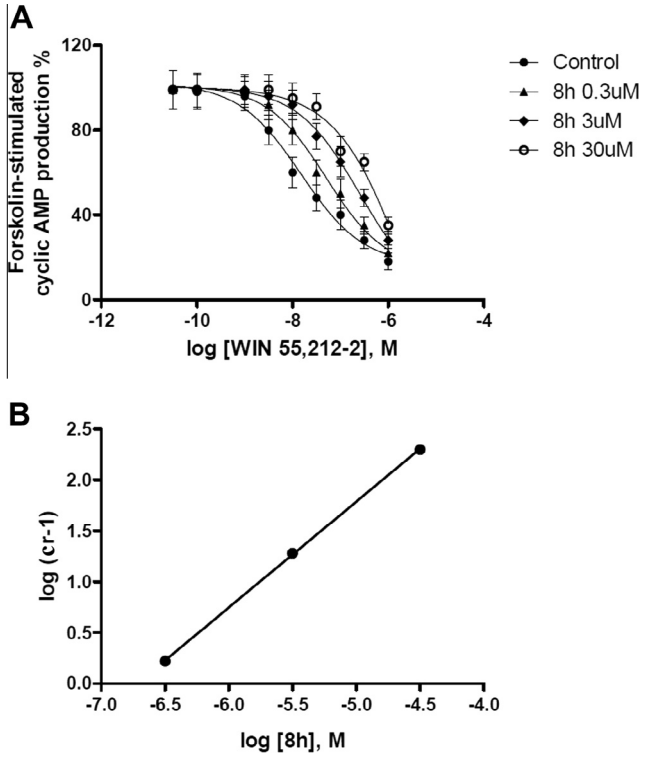

Figure 5. (A) Concentration–response curves of WIN 55,212-2 in hCB_2CHO cells in the absence and presence of various concentrations of **8h**. (B) Schild plot of **8h** against WIN 55,212-2. Abscissa, log of the molar concentration of the antagonist **8h**. Ordinate, log of the concentration ratio −1 (cr −1) of the agonist WIN 55,212-2. Values are the mean ± SEM of four independent experiments ($N = 4$).

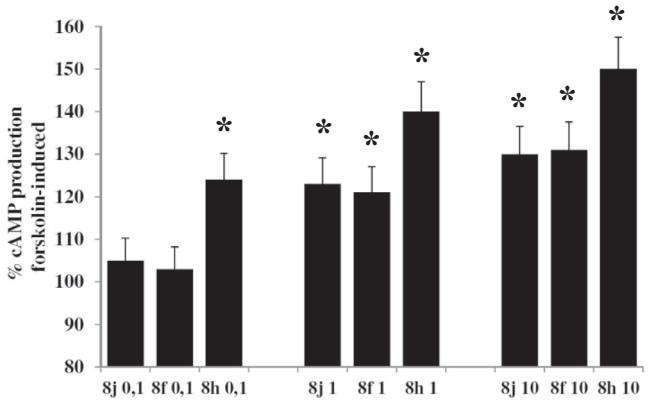

Figure 6. Effect of **8j**, **8f**, and **8h** (0.1–10 μM) expressed as% of increase of forskolin-stimulated cAMP accumulation (100%) in hCB_2CHO cells. Forskolin (10 μM) effect was set to 100%. Values are the mean ± SEM of four independent experiments ($N = 4$). $^{*}P < 0.05$, compared with Forskolin (10 μM); analysis was by ANOVA followed by Dunnett's test.

number of π–π stacking and Van der Waals contacts with the three aforementioned hydrophobic pockets (see Supplementary data, Fig. 9). More in details, the most potent **8h** derivative shows one H-bond between the carbonyl oxygen atom and the S165 side-chain, in tandem with a second H-bond with the T114 backbone (Fig. 7).

In addition, the phenyl ring is engaged in π–π stacking with W194 while the tricyclic core proves to mimic the reference compound fenchyl group. Accordingly, **8h** is characterized by a very favorable selectivity profile. Furthermore, the Q substituent is able to play the same role of the SR144528 phenyl and benzyl substituents, partially occupying the region delimited by L107, I110, L169, L182 and Y190.

As shown in Figures 8 and 9, the related analogues **8f** and **8j** display a highly similar binding mode, with the exception of the Q group on **8j**. Indeed, the presence of a methylene between the nitrogen atom and the cycloaliphatic moiety increases the Q group flexibility, thus it moves quite far from the receptor crevice surrounded by L107, I110 and L182.

These results confirm that a promising affinity profile could be obtained especially performing a proper set of H-bonds with T114

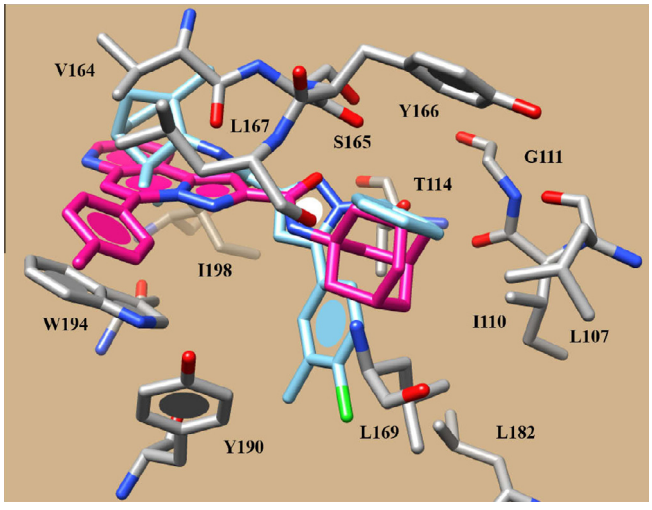

Figure 7. SR144528 (C atom: cyan) and compound **8h** (C atom: deep magenta) docking poses into the hCB_2 inverse agonist binding site. The most important residues are labeled.

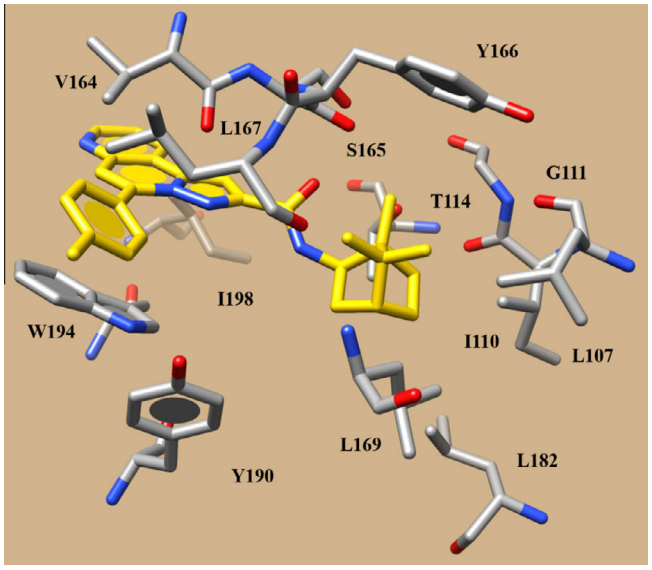

Figure 8. Docking poses of compound **8f** (C atom: yellow) within the hCB_2 inverse agonist binding site. The most important residues are labeled.

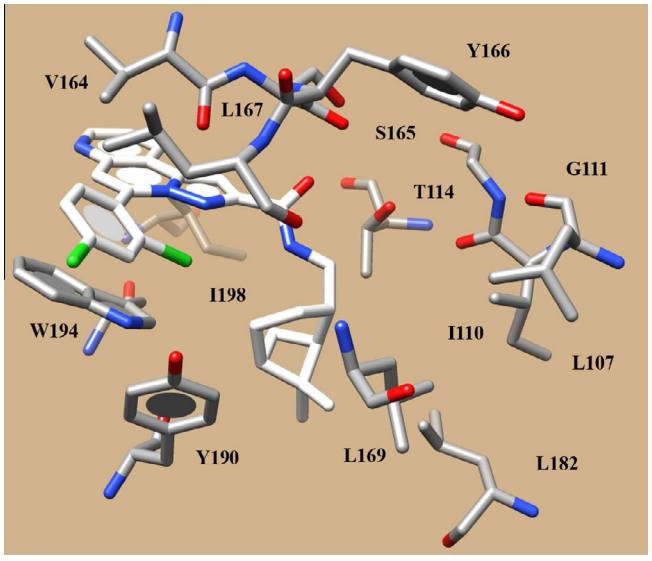

Figure 9. Docking poses of compound **8j** (C atom: white) within the hCB_2 inverse agonist binding site. The most important residues are labeled.

and S165, while selectivity appears to be strictly related to the hindered groups interacting with V164. On this basis, the computational studies here discussed are expected to pave the way for a further design process and for the filtering of new more potent and selective ligands.

3.4. In silico evaluation of pharmacokinetic properties

The computationally-driven prediction of descriptors related to absorption, distribution, metabolism, excretion and toxicity properties (ADMET) allows to rely on a useful strategy accelerating the lead compound discovery process.[41]

In this work, for the newly synthesized derivatives **8f**, **8h**, **8j** and also for **4**, a series of ADMET properties were calculated. In details, we took into account the logarithmic ratio of the octanol–water partitioning coefficient (*c*Log*P*), extent of blood–brain barrier permeation (Log BB), rate of passive diffusion-permeability (Log PSA),

human intestinal absorption (HIA), volume of distribution (Vd), the role played by plasmatic protein binding (%PPB) and by the compound affinity toward the human serum albumin ($\mathrm{Log}K_a^{HSA}$), and an overall perspective of the molecule oral bioavailability (%F).

In addition, we evaluated a number of descriptors predicting for metabolism and toxicity profiles, including the compound potential behavior as P-glycoprotein substrate, the ability to act as cytochrome P450 3A4 inhibitor or substrate, the median lethal dose (LD_{50}) related to oral administration.

As shown in Table 2, all the compounds are characterized by a better favorable profile in terms of lipophilicity, being the calculated *c*Log*P* within 5 (Lipinski rules) for **8f** and **8h** and, in any case, lower than that displayed by the reference compound **4**, being insoluble in water (solubility $\leqslant$ 0.05 mg/mL). Notably, all of them, with the exception of **8j**, show an overall adequate blood–brain barrier permeation, showing Log BB and/or Log PSA values falling in the recommended ranges ($0 < \mathrm{Log\,BB} < 1.5$; $-3 < \mathrm{Log\,PSA} < -1$). Only **8j** was characterized by a predicted weak ability to pass at the central nervous system. All of them are able to be fully adsorbed at the human intestinal membrane (HIA). The calculated volume of distribution values and the potential binding to the plasmatic proteins fall in the allowed ranges, being in any case consistent with those shown for **4**. As an overall consequence, compounds **8f** and **8h** are endowed with a favorable or acceptable bioavailability profile (%F), especially in comparison with **4**.

Based on Table 3, none of the compounds here proposed should be substrate of the P-glycoprotein, or be involved in cytochrome P450 3A4 inhibition. On the contrary, they should be substrate for the enzyme, showing comparable values with those displayed by **4**. Finally, **8f** and **8h** exhibit an acceptable toxicity profile, being the estimated LD_{50} in the range of 320–430 mg/kg for mouse after oral administration, a value highly comparable with that calculated for the reference compound.

4. Conclusion

In conclusion, a small series of pyrazolo[5,1-*f*][1,6]naphthyridines **8** have been designed and synthesized for CB_1/CB_2R interaction. Among the synthesized compounds, **8f**, **8h** and **8j** exhibited affinity levels for CB_2R in the near nM range (33–67 nM) with a high degree of selectivity for CB_2 compared to CB_1 (K_iCB_1/K_iCB_2: 132–173). According to in vitro assays based on the effects of forskolin-stimulated cAMP levels in human CB_2 CHO cells, compounds **8f**, **8h** and **8j** act as antagonist/inverse agonists. Docking studies carried out on such compounds and the reference **4** (SR144528) disclosed the specific pattern of interactions probably related to the pyrazolo[5,1-*f*][1,6]naphthyridine scaffold as CB_2 inverse agonists. Our preliminary results point out the versatility of the planar pyrazolo[5,1-*f*][1,6]naphthyridine architecture to provide novel chemical entities for CB_2R interaction and pave the way for a further design process and for the filtering of new more potent and selective CB_2 ligands. Further work on this interesting class of CB_2R ligands will be disclosed in due course.

5. Experimental protocols

5.1. Chemistry

5.1.1. General methods

Melting points were obtained on a Koffler melting point apparatus and are uncorrected. IR spectra were recorded as KBr pellets with a Jasco FT/IR 460 plus spectrophotometer and are expressed in ν (cm^{-1}). ^1H NMR spectra were taken on a Bruker AVANCE III Nanobody 400 MHz spectrometer with ^1H and ^{13}C being observed at 400 and 100.6 MHz, respectively. Chemical shifts for ^1H and ^{13}C NMR spectra were reported in δ (ppm) downfield from tetramethylsilane, and coupling constants (*J*) were expressed in Hertz. Multiplicities are recorded as s (singlet), br s (broad singlet), d (doublet), t (triplet), dd (doublet of doublets), ddd (doublet of doublet douplets), m (multiplet). Atmospheric Pressure Ionization Electrospray (API-ES) mass spectra were obtained on an Agilent 1100 series LC/MSD spectrometer. Elemental analyses were performed with a PerkineElmer 2400 analyzer, and results were within ±0.40% of the calculated values. Microwave experiments were carried out by a Biotage Iniziator-8-microwave system (max pressure 20 bar, IR temperature sensor). TLC was performed on Merck silica gel 60 TLC plates F254 and visualized using UV. Flash chromatography (FC) was performed using Merck silica gel 60 (230–400 mesh ASTM).

2-Bromonicotinaldehyde (**9**), amines and *p*-tolylacetylene were purchased by Sigma–Aldrich®. Fenchylamine[42] and 2,4-dichlorophenylacetylene[43] were synthesized according to literature procedure. Title compounds **8a**, **8h** and **8i** were tested as hydrochloride salts.

5.1.2. General procedure I. Synthesis of o-alkynylaldehydes (10,11)

A mixture of 2-bromonicotinaldehyde (**9**) (1 equiv, 2.68 mmol), the appropriate alkyne (1.2 equiv, 3.22 mmol), $Pd(PPh_3)_2Cl_2$ (0.04 equiv, 0.11 mmol), CuI (0.07 equiv, 0.20 mmol), Et_3N (1.5 equiv, 4.02 mmol), in dry DMF (16 mL), was stirred under argon atmosphere using microwave irradiation at 60 °C for 20 min. The reaction mixture was cooled to room temperature, quenched with Et_2O (200 mL) and the solid filtered off. The organic solution was evaporated to afford a crude residue which was purified by FC (petroleum ether/AcOEt 8:2).

5.1.2.1. 2-(*p*-Tolylethynyl)nicotinaldehyde (10).[44] General procedure I was used to convert **9** and *p*-tolylacetylene into the title product. Yellow solid (0.485 g, 82%); R_f 0.37 (AcOEt/petroleum ether 2:8); mp 97–99 °C (96–100 °C); ^1H NMR ($CDCl_3$) 2.39 (s, 3H), 7.20 (d, J = 7.6 Hz, 2H), 7.38 (dd, J = 4.8 Hz, J = 7.6 Hz, 1H), 7.63 (d, J = 7.6 Hz, 2H), 8.20 (d, J = 8.0 Hz, 1H), 8.81 (d, J = 4.8 Hz, 1H), 10.66 (s, 1H); ^{13}C NMR ($CDCl_3$) 21.8, 84.4, 96.7, 118.3, 123.2, 129.5, 131.8, 132.3, 134.9, 140.5, 146.4, 154.6, 191.1; API-ES *m/z*: $[M+H]^+$ calcd for $C_{15}H_{12}NO$: 222.1, found: 222.1.

5.1.2.2. 2-((2,4-Dichlorophenyl)ethynyl)nicotinaldehyde (11). General procedure I was used to convert **9** and 2,4-dichlorophenylacetylene into the title product. Cream solid (0.376 g, 51%); R_f 0.28 (AcOEt/petroleum ether 2:8); mp 160–162 °C; ^1H NMR ($CDCl_3$) 7.29 (dd, J = 1.6 Hz, J = 8.4 Hz, 1H,), 7.44 (dd, J = 4.8 Hz, J = 8.0 Hz, 1H), 7.49 (d, J = 1.6 Hz, 1H), 7.62 (d, J = 8.4 Hz, 1H), 8.23 (dd, J = 1.2 Hz, J = 8.0 Hz, 1H), 8.84 (dd, J = 1.6 Hz, J = 4.8 Hz, 1H), 10.73 (s, 1H); ^{13}C NMR ($CDCl_3$) 90.3, 91.4, 120.2, 123.8, 127.5, 129.8, 132.4, 134.7, 134.9, 136.6, 137.6, 145.6, 154.7, 190.9; API-ES *m/z*: $[M+H]^+$ calcd for $C_{14}H_8Cl_2NO$: 275.9, found: 275.8. Anal. ($C_{14}H_7Cl_2NO$) C, H, N.

5.1.3. General procedure II. Synthesis of pyrazole esters (12,13)

A mixture of the appropriate *o*-alkynylaldehyde (1 equiv, 0.452 mmol), PTSH (1.05 equiv, 0.474 mmol), AgOTf (0.1 equiv, 0.0452 mmol), DL-proline (0.1 equiv, 0.0452 mmol), in dry EtOH (4 mL) was stirred at room temperature for 10 min. Ethyl pyruvate (10 equiv, 4.520 mmol) was added, and the whole heated by microwave irradiation to 60 °C for 3.5 h. The reaction mixture was cooled to room temperature; Na_2CO_3 (6 equiv, 2.712 mmol) was added and the mixture stirred at room temperature for 12 h. The solvent was evaporated to afford a crude residue which was purified by FC (petroleum ether/AcOEt 6:4).

Table 2
Calculated ADMET descriptors related to absorption and distribution properties

Compd	*c*Log *P*	Log BB[a]	Log PSA[b]	HIA (%)[c]	Vd (l/kg)[d]	%PPB	Log Ka^{HSA}	%F (oral)
8f	5.00	0.44	−1.1	100	2.7	97.92	4.68	97.3
8h	4.89	0.27	−1.1	100	2.7	98.26	4.94	78.6
8j	6.12	0.00	−1.3	100	3.6	99.00	5.47	34.6
SR144528 (4)	6.19	0.37	−1.3	100	4.0	98.96	5.39	89.0

[a] Extent of brain penetration based on ratio of total drug concentrations in tissue and plasma at steady-state conditions.
[b] Rate of passive diffusion-permeability. PSA represents Permeability-Surface area product and is derived from the kinetic equation of capillary transport.
[c] HIA represents the human intestinal absorption, expressed as percentage of the molecule able to pass through the intestinal membrane.
[d] Prediction of volume of distribution (Vd) of the compound in the body.

Table 3
Calculated ADMET descriptors related to metabolism, excretion and toxicity properties

Compd	P-glycoprotein substrate (R.I. ⩾ 0.40)	CYP3A4		LD_{50} (mg/kg)[a] (R.I. ⩾ 0.40)
		Inhibitor (IC_{50} < 10 μM) (R.I. ⩾ 0.40)	Substrate (R.I. ⩾ 0.40)	
8f	Not	0.50	0.99	430
8h	Not	0.32	0.98	320
8j	Not	0.21	0.98	270
SR144528 (4)	Not	0.39	0.99	440

[a] Acute toxicity (LD_{50}) for mouse after oral administration (RI: reliability index). Borderline-allowed values for reliability parameter are ⩾0.3, the most predictive fall in the range 0.50–1.

5.1.3.1. Ethyl 5-(*p*-tolyl)pyrazolo[5,1-*f*][1,6]naphthyridine-2-carboxylate (12). General procedure II was used to convert **10** into the title product. White solid (0.100 g, 64%); R_f 0.34 (AcOEt/petroleum ether 4:6); mp 176–179 °C; IR 1716 (CO); ^{1}H NMR ($CDCl_3$) 1.44 (t, *J* = 7.2 Hz, 3H), 2.46 (s, 3H), 4.46 (q, *J* = 7.2 Hz, 2H), 7.35 (d, *J* = 8.0 Hz, 2H), 7.46 (s, 1H), 7.50 (dd, *J* = 4.8 Hz, *J* = 8.0 Hz, 1H), 7.66 (s, 1H), 7.90 (d, *J* = 8.0 Hz, 2H), 8.40 (dd, *J* = 1.6 Hz, *J* = 8.0 Hz, 1H), 8.90 (dd, *J* = 1.6 Hz, *J* = 4.8 Hz, 1H); ^{13}C NMR ($CDCl_3$) 14.5, 21.6, 61.5, 102.0, 115.8, 119.8, 122.3, 129.4, 129.6, 129.7, 131.3, 139.7, 140.4, 142.6, 145.1, 146.4, 151.4, 162.7; API-ES *m/z*: $[M+H]^+$ calcd for $C_{20}H_{18}N_3O_2$: 332.1, found: 332.1. Anal. ($C_{20}H_{17}N_3O_2$) C, H, N.

5.1.3.2. Ethyl 5-(2,4-dichlorophenyl)pyrazolo[5,1-*f*][1,6]naphthyridine-2-carboxylate (13). General procedure II was used to convert **11** into the title product. White solid (0.085 g, 49%); R_f 0.31 (AcOEt/petroleum ether 4:6); mp 231–234 °C; IR 1729 (CO); ^{1}H NMR (DMSO-d_6) 1.31 (t, *J* = 6.4 Hz, 3H), 4.34 (q, *J* = 6.4 Hz, 2H), 7.49 (s, 1H), 7.68 (d, *J* = 8.0 Hz, 1H), 7.77 (d, *J* = 8.0 Hz, 2H), 7.91 (s, 1H), 8.06 (s, 1H), 8.91–9.00 (m, 2H); ^{13}C NMR (DMSO-d_6) 14.2, 60.9, 103.1, 117.3, 119.9, 123.6, 127.8, 129.2, 130.7, 132.2, 133.5, 134.6, 135.5, 137.7, 138.7, 144.5, 144.8, 151.7, 161.6; API-ES *m/z*: $[M+H]^+$ calcd for $C_{19}H_{14}Cl_2N_3O_2$: 386.0, found: 386.3. Anal. ($C_{19}H_{13}Cl_2N_3O_2$) C, H, N.

5.1.4. General procedure III. Synthesis of pyrazole acids (14,15)

To a solution of appropriate pyrazole ester (1 equiv, 1.41 mmol) in THF (10 mL), 10% aqueous NaOH solution (10 mL) was added dropwise, and the whole stirred at 40 °C for 3 h. The solution was cooled at room temperature and neutralized with 4N HCl. The solid was filtered, washed with acetone to give a crude product which was used in the following step with no further purification.

5.1.4.1. 5-(*p*-Tolyl)pyrazolo[5,1-*f*][1,6]naphthyridine-2-carboxylic acid (14). General procedure III was used to convert **12** into the title product. White solid (0.443 g, 95%). IR 3422 (OH), 1636 (CO).

5.1.4.2. 5-(2,4-Dichlorophenyl)pyrazolo[5,1-*f*][1,6]naphthyridine-2-carboxylic acid (15). General procedure III was used to convert **13** into the title product. Yellow solid (0.352 g, 70%). IR 3448 (OH), 1718 (CO).

5.1.5. General procedure IV. Synthesis of carboxamides (8a–k)

A solution of appropriate acid (1 equiv. 0.495 mmol) and Et_3N (3 equiv. 1.50 mmol) in dry CH_2Cl_2 (10 mL) was cooled at 0 °C; pivaloyl chloride (2.5 equiv. 1.237 mmol) was dropwise added and the whole warmed to room temperature and stirred for 2 h. This mixture was dropwise added at 0 °C to a solution of appropriate amine or hydrazine (0.9 equiv. 0.990 mmol) and Et_3N (1.5 equiv. 1.500 mmol) in dry CH_2Cl_2 (5 mL) and the whole stirred at room temperature for 2.5 h. The reaction mixture was quenched with an aqueous saturated solution of NH_4Cl and extracted with CH_2Cl_2. The organic phase was dried (Na_2SO_4) and evaporated to give a crude residue which was purified by FC (petroleum ether/AcOEt 3:7).

5.1.5.1. *N*-Fenchyl-5-(*p*-tolyl)pyrazolo[5,1-*f*][1,6]naphthyridine-2-carboxamide (8a). General procedure IV was used to convert **14** and fenchylamine into the title product. White solid (0.050 g, 23%). R_f 0.49 (AcOEt/petroleum ether 7:3); mp 220–222 °C; IR 3404 (NH), 1673 (CO); ^{1}H NMR ($CDCl_3$) 0.86 (s, 3H), 1.11 (s, 3H), 1.14–1.22 (m, 4H), 1.23–1.30 (m, 1H), 1.29–1.39 (m, 1H), 1.43–1.55 (m, 1H), 1.66–1.77 (m, 2H), 1.80 (d, *J* = 2.8 Hz, 1H), 2.49 (s, 3H), 3.83 (d, *J* = 9.6 Hz, 1H), 7.23 (d, *J* = 9.6 Hz, 1H), 7.36 (d, *J* = 8.0 Hz, 2H), 7.46 (s, 1H), 7.50 (dd, *J* = 4.4 Hz, *J* = 8.0 Hz, 1H), 7.65 (s, 1H), 7.93 (d, *J* = 8.0 Hz, 2H), 8.42 (d, *J* = 8.0 Hz, 1H), 8.89 (d, *J* = 4.4 Hz, 1H); ^{13}C NMR ($CDCl_3$) 19.8, 21.3, 21.7, 26.1, 27.3, 31.1, 39.7, 42.8, 48.3, 48.9, 63.3, 99.7, 115.2, 119.9, 122.4, 129.0, 129.6, 129.8, 131.5, 140.2, 140.4, 141.9, 146.4, 147.9, 151.3, 162.5; API-ES *m/z*: $[M+H]^+$ calcd for $C_{28}H_{31}N_4O$: 439.2, found: 439.2. Anal. ($C_{28}H_{30}N_4O$) C, H, N.

5.1.5.2. *N*-(piperidin-1-yl)-5-(*p*-tolyl)pyrazolo[5,1-*f*][1,6]naphthyridine-2-carboxamide (8b). General procedure IV was used to convert **14** and *N*-aminopiperidine into the title product. Cream solid (0.078 g, 41%). R_f 0.11 (AcOEt/petroleum ether 7:3); mp 207 °C; IR 3398 (NH), 1687 (CO); ^{1}H NMR ($CDCl_3$) 1.41–1.49 (m, 2H), 1.71–1.79 (m, 4H), 2.50 (s, 3H), 2.90 (t, *J* = 5.2 Hz, 4H), 7.39 (d, *J* = 8.0 Hz, 2H), 7.41 (s, 1H), 7.51 (dd, *J* = 4.4 Hz, *J* = 8.0 Hz, 1H), 7.72 (s, 1H), 7.76 (s, 1H), 7.84 (d, *J* = 8.0 Hz, 2H), 8.41 (dd, *J* = 1.6 Hz, *J* = 8.0 Hz, 1H), 8.89 (dd, *J* = 1.6 Hz, *J* = 4.4 Hz, 1H); ^{13}C NMR ($CDCl_3$) 21.7, 23.4, 25.5, 57.0, 100.6, 115.6, 119.8, 122.5, 129.3, 129.5, 129.9, 131.6, 140.0, 140.4, 142.0, 146.3, 147.3,

151.4, 159.3; API-ES *m/z*: $[M+H]^+$ calcd for $C_{23}H_{24}N_5O$: 386.2, found: 386.0. Anal. ($C_{23}H_{23}N_5O$) C, H, N.

5.1.5.3. *N*-Cyclohexyl-5-(*p*-tolyl)pyrazolo[5,1-*f*][1,6]naphthyridine-2-carboxamide (8c). General procedure IV was used to convert **14** and *N*-cyclohexylamine into the title product. White solid (0.051 g, 27%). R_f 0.50 (AcOEt/petroleum ether 7:3); mp 229–230 °C; IR 3406 (NH), 1670 (CO); ^{1}H NMR ($CDCl_3$) 1.16–1.32 (m, 3H), 1.35–1.48 (m, 2H), 1.60–1.69 (m, 1H), 1.71–1.80 (m, 2H), 1.97–2.06 (m, 2H), 2.49 (s, 3H), 3.92–4.05 (m, 1H), 6.89 (d, *J* = 8.0 Hz, 1H), 7.38 (d, *J* = 8.0 Hz, 2H), 7.40 (s, 1H), 7.50 (dd, *J* = 4.8 Hz, *J* = 8.0 Hz, 1H), 7.67 (s, 1H), 7.85 (d, *J* = 8.0 Hz, 2H), 8.41 (d, *J* = 8.0 Hz, 1H), 8.88 (d, *J* = 3.20 Hz, 1H); ^{13}C NMR ($CDCl_3$) 21.6, 25.1, 25.7, 33.3, 48.3, 100.1, 115.4, 119.9, 122.4, 129.3, 129.5, 129.9, 131.5, 140.1, 140.3, 142.1, 146.3, 148.2, 151.3, 161.0; API-ES *m/z*: $[M+H]^+$ calcd for $C_{24}H_{25}N_4O$: 385.2, found: 385.5. Anal. ($C_{24}H_{24}N_4O$) C, H, N.

5.1.5.4. *N*-Myrtanyl-5-(*p*-tolyl)pyrazolo[5,1-*f*][1,6]naphthyridine-2-carboxamide (8d). General procedure IV was used to convert **14** and myrtanylamine into the title product. White solid (0.128, 59%). R_f 0.53 (AcOEt/petroleum ether 7:3); mp 164–166 °C; IR 3448 (NH), 1670 (CO); ^{1}H NMR ($CDCl_3$) 0.91 (d, *J* = 9.6 Hz, 1H), 1.10 (s, 3H), 1.21 (s, 3H), 1.51–1.62 (m, 1H); 1.85–2.01 (m, 5H), 2.28–2.40 (m, 2H), 2.49 (s, 3H), 3.41–3.53 (m, 2H), 7.08 (t, *J* = 5.8 Hz, 1H), 7.38 (d, *J* = 8.0 Hz, 2H), 7.41 (s, 1H), 7.51 (dd, *J* = 4.0 Hz, *J* = 8.0 Hz, 1H), 7.68 (s, 1H), 7.85 (d, *J* = 8.0 Hz, 2H), 8.42 (dd, *J* = 0.8 Hz, *J* = 8.0 Hz, 1H), 8.89 (d, *J* = 3.2 Hz, 1H); ^{13}C NMR ($CDCl_3$) 19.9, 21.66, 23.4, 26.2, 28.1, 33.4, 38.9, 41.5, 41.7, 44.0, 44.9, 100.1, 115.4, 119.9, 122.4, 129.3, 129.6, 129.9, 131.6, 140.1, 140.4, 142.1, 146.3, 148.0, 151.3, 161.9; API-ES *m/z*: $[M+H]^+$ calcd for $C_{28}H_{31}N_4O$: 439.2, found: 439.5. Anal. ($C_{28}H_{30}N_4O$) C, H, N.

5.1.5.5. *N*-Isopinocampheyl-5-(*p*-tolyl)pyrazolo[5,1-*f*][1,6]naphthyridine-2-carboxamide (8e). General procedure IV was used to convert **14** and isopinocampheylamine into the title product. Yellow solid (0.074 g, 34%). R_f 0.40 (AcOEt/petroleum ether 7:3); mp 215 °C; IR 3402 (NH), 1662 (CO); ^{1}H NMR ($CDCl_3$) 0.95 (d, *J* = 10.0 Hz, 1H), 1.11 (s, 3H), 1.17 (d, *J* = 7.2 Hz, 3H), 1.25 (s, 3H), 1.68 (ddd, *J* = 2.0 Hz, *J* = 6.0 Hz, *J* = 14.0 Hz, 1H), 1.87 (t, *J* = 5.6 Hz, 1H), 1.93 (t, *J* = 7.0 Hz, 1H), 1.96–2.02 (m, 1H), 2.40–2.48 (m, 1H), 2.50 (s, 3H), 2.63–2.73 (m, 1H), 4.45–4.56 (m, 1H), 6.89 (d, *J* = 9.2 Hz, 1H), 7.39 (d, *J* = 8.0 Hz, 2H), 7.42 (s, 1H), 7.51 (dd, *J* = 4.0 Hz, *J* = 8.0 Hz, 1H), 7.69 (s, 1H), 7.87 (d, *J* = 8.0 Hz, 2H), 8.43 (d, *J* = 8.0 Hz, 1H), 8.90 (d, *J* = 4.0 Hz, 1H); ^{13}C NMR ($CDCl_3$) 21.0, 21.7, 23.6, 28.2, 35.3, 37.1, 38.6, 41.8, 46.2, 47.9, 48.0, 100.2, 115.5, 119.9, 122.4, 129.3, 129.5, 129.9, 131.5, 140.1, 140.4, 142.1, 146.3, 148.1, 151.3, 161.4; API-ES *m/z*: $[M+H]^+$ calcd for $C_{28}H_{31}N_4O$: 439.2, found: 439.4. Anal. ($C_{28}H_{30}N_4O$) C, H, N.

5.1.5.6. *N*-Bornyl-5-(*p*-tolyl)pyrazolo[5,1-*f*][1,6]naphthyridine-2-carboxamide (8f). General procedure IV was used to convert **14** and bornylamine into the title product. Yellow solid (0.093 g, 43%). R_f 0.52 (AcOEt/petroleum ether 7:3); mp 224–225 °C; IR 3390 (NH), 1676 (CO); ^{1}H NMR ($CDCl_3$) 0.90 (s, 3H), 0.91 (s, 3H), 0.95 (dd, *J* = 4.4 Hz, *J* = 13.6 Hz, 1H), 1.01 (s, 3H), 1.18–1.28 (m, 1H), 1.38–1.50 (m, 1H), 1.55–1.65 (m, 1H), 1.71 (t, *J* = 4.4 Hz, 1H), 1.76–1.88 (m, 1H), 2.37–2.47 (m, 1H), 2.49 (s, 3H), 4.41–4.50 (m, 1H), 7.17 (d, *J* = 9.2 Hz, 1H), 7.37 (d, *J* = 8.0 Hz, 2H), 7.45 (s, 1H), 7.51 (dd, *J* = 4.4 Hz, *J* = 8.0 Hz, 1H), 7.66 (s, 1H), 7.92 (d, *J* = 8.0 Hz, 2H), 8.42 (d, *J* = 8.0 Hz, 1H), 8.90 (dd, *J* = 1.2 Hz, *J* = 4.4 Hz, 1H);); ^{13}C NMR ($CDCl_3$): 13.9, 18.9, 20.0, 21.7, 28.2, 28.5, 37.7, 45.2, 48.3, 50.0, 53.7, 99.9, 115.2, 119.9, 122.4, 129.1, 129.6, 129.8, 131.6, 140.2, 140.5, 142.0, 146.4, 148.0, 151.3, 162.0; API-ES *m/z*: $[M+H]^+$ calcd for $C_{28}H_{31}N_4O$: 439.2, found: 439.2. Anal. ($C_{28}H_{30}N_4O$) C, H, N.

5.1.5.7. *N*-Menthyl-5-(*p*-tolyl)pyrazolo[5,1-*f*][1,6]naphthyridine-2-carboxamide (8g). General procedure IV was used to convert **14** and menthylamine into the title product. White solid (0.165 g, 76%). R_f 0.58 (AcOEt/petroleum ether 7:3); mp 151–152 °C; IR 3399 (NH), 1664 (CO); ^{1}H NMR ($CDCl_3$) 0.85–0.93 (m, 11H), 1.11–1.23 (m, 2H), 1.49–1.60 (m, 1H), 1.66–1.77 (m, 2H), 1.88–2.01 (m, 1H), 2.02–2.11 (m, 1H), 2.50 (s, 3H), 3.93–4.05 (m, 1H), 6.75 (d, *J* = 9.6 Hz, 1H), 7.38 (d, *J* = 8.0 Hz, 2H), 7.41 (s, 1H), 7.51 (dd, *J* = 4.4 Hz, *J* = 8.0 Hz, 1H), 7.68 (s, 1H), 7.86 (d, *J* = 8.0 Hz, 2H), 8.41 (d, *J* = 8.0 Hz, 1H), 8.89 (d, *J* = 4.4 Hz, 1H); ^{13}C NMR ($CDCl_3$) 16.8, 21.1, 21.7, 22.3, 24.5, 27.3, 32.1, 34.7, 43.1, 48.2, 50.1, 100.1, 115.4, 119.9, 122.4, 129.3, 129.5, 130.0, 131.5, 140.1, 140.3, 142.1, 146.3, 148.1, 151.3, 161.2; API-ES *m/z*: $[M+H]^+$ calcd for $C_{28}H_{33}N_4O$: 441.2, found: 441.5. Anal. ($C_{28}H_{32}N_4O$) C, H, N.

5.1.5.8. *N*-Adamant-1-yl-5-(*p*-tolyl)pyrazolo[5,1-*f*][1,6]naphthyridine-2-carboxamide (8h). General procedure IV was used to convert **14** and 1-adamantylamine into the title product. White solid (0.12 g, 55%). R_f 0.54 (AcOEt/petroleum ether 7:3); mp 238–240 °C; IR 3390 (NH), 1676 (CO); ^{1}H NMR ($CDCl_3$) 1.68–1.77 (m, 6H), 2.10–2.18 (m, 9H), 2.48 (s, 3H), 6.80 (s, 1H), 7.37 (d, *J* = 8.0 Hz, 2H), 7.39 (s, 1H), 7.49 (dd, *J* = 4.4 Hz, *J* = 8.0 Hz, 1H), 7.61 (s, 1H), 7.85 (d, *J* = 8.0 Hz, 2H), 8.40 (d, *J* = 8.0 Hz, 1H), 8.88 (d, *J* = 4.4 Hz, 1H); ^{13}C NMR ($CDCl_3$) 21.6, 29.6, 36.5, 41.7, 52.1, 99.8, 115.2, 119.9, 122.3, 129.2, 129.6, 129.9, 131.5, 140.1, 140.3, 142.0, 146.3, 148.9, 151.2, 160.9; API-ES *m/z*: $[M+H]^+$ calcd for $C_{28}H_{29}N_4O$: 437.2, found: 437.5. Anal. ($C_{28}H_{28}N_4O$) C, H, N.

5.1.5.9. *N*-Adamant-2-yl-5-(*p*-tolyl)pyrazolo[5,1-*f*][1,6]naphthyridine-2-carboxamide (8i). General procedure IV was used to convert **14** and 2-adamantylamine hydrochloride into the title product. White solid (0.153 g, 71%). R_f 0.39 (AcOEt/petroleum ether 7:3); mp 218–220 °C; IR 3419 (NH), 1672 (CO); ^{1}H NMR ($CDCl_3$) 1.68 (d, *J* = 12.8 Hz, 2H), 1.78 (s, 2H), 1.83–1.92 (m, 8H), 2.05 (s, 2H), 2.48 (s, 3H), 4.26 (d, *J* = 8.0 Hz, 1H), 7.36 (d, *J* = 8.0 Hz, 2H), 7.44 (s, 1H), 7.46–7.54 (m, 2H), 7.66 (s, 1H), 7.91 (d, *J* = 8.0 Hz, 2H), 8.41 (d, *J* = 8.0 Hz, 1H), 8.88 (d, *J* = 4.4 Hz, 1H); ^{13}C NMR ($CDCl_3$) 21.6, 27.3, 27.5, 32.1, 32.2, 37.2, 37.7, 53.2, 99.8, 115.2, 119.9, 122.3, 129.1, 129.6, 129.8, 131.5, 140.1, 140.4, 142.0, 146.4, 148.1, 151.3, 161.0; API-ES *m/z*: $[M+H]^+$ calcd for $C_{28}H_{29}N_4O$: 437.2, found: 437.4. Anal. ($C_{28}H_{28}N_4O$) C, H, N.

5.1.5.10. *N*-Myrtanyl-5-(2,4-dichlorophenyl)pyrazolo[5,1-*f*][1,6]naphthyridine-2-carboxamide (8j). General procedure IV was used to convert **15** and myrtanylamine into the title product. White solid (0.090 g, 37%). R_f 0.38 (AcOEt/petroleum ether 6:4); mp 216–218 °C; IR 3403 (NH), 1687 (CO); ^{1}H NMR ($CDCl_3$) 0.90 (d, *J* = 9.6 Hz, 1H), 1.09 (s, 3H), 1.19 (s, 3H), 1.49–1.61 (m, 1H), 1.80–2.0 (m, 5H), 2.26–2.39 (m, 2H), 3.40–3.51 (m, 2H), 6.93 (t, *J* = 6.0 Hz, 1H), 7.36 (s, 1H), 7.46 (d, *J* = 8.4 Hz, 1H), 7.51–7.60 (m, 2H), 7.63 (s, 1H), 7.67 (s, 1H), 8.45 (d, *J* = 8.4 Hz, 1H), 8.92 (d, *J* = 4.4 Hz, 1H); ^{13}C NMR ($CDCl_3$) 19.8, 23.4, 26.2, 28.1, 33.3, 38.8, 41.5, 41.6, 44.0, 45.0, 100.2, 117.2, 120.6, 123.0, 127.5, 130.1, 130.8, 131.7, 132.8, 135.6, 136.6, 138.4, 139.4, 145.7, 148.4, 151.4, 161.8; API-ES *m/z*: $[M+H]^+$ calcd for $C_{27}H_{27}Cl_2N_4O$: 493.2, found: 493.3. Anal. ($C_{27}H_{26}Cl_2N_4O$) C, H, N.

5.1.5.11. *N*-Fenchyl-5-(2,4-dichlorophenyl)pyrazolo[5,1-*f*][1,6]-naphthyridine-2-carboxamide (8k). General procedure IV was used to convert **15** and fenchylamine into the title product. Cream solid (0.011 g, 44%). R_f 0.42 (AcOEt/petroleum ether 6:4); mp 249–251 °C; IR 3387 (NH), 1671 (CO); ^{1}H NMR ($CDCl_3$) 0.78

(s, 3H), 1.07 (s, 3H), 1.12–1.22 (m, 5H), 1.42–1.53 (m, 1H), 1.55–1.62 (m, 1H), 1.63–1.73 (m, 2H), 1.75–1.82 (m, 1H), 3.78 (d, J = 9.6 Hz, 1H), 7.07 (d, J = 10.0 Hz, 1H), 7.39 (s, 1H), 7.46 (d, J = 8.4 Hz, 1H), 7.54–7.60 (m, 2H), 7.62 (s, 1H), 7.65 (s, 1H), 8.46 (d, J = 8.4 Hz, 1H), 8.93 (d, J = 4.4 Hz, 1H); ^{13}C NMR ($CDCl_3$): 19.8, 21.6, 26.1, 27.3, 31.1, 39.7, 42.7, 48.3, 48.9, 63.4, 99.9, 117.2, 120.6, 123.0, 127.4, 129.8, 130.8, 131.7, 132.8, 133.0, 136.7, 138.5, 139.4, 145.8, 148.4, 151.4, 162.3; API-ES m/z: $[M+H]^+$ calcd for $C_{27}H_{27}Cl_2N_4O$: 493.2, found: 493.4. Anal. ($C_{27}H_{26}Cl_2N_4O$) C, H, N.

5.2. Biological evaluation

5.2.1. Competition binding experiments for human CB_1 and CB_2 receptors

Competition binding experiments were carried out through [^{3}H] CP-55,940 (specific activity, 180 Ci/mmol) provided by Perkin-Elmer Life and Analytical Sciences (U.S.). Human CB_1 and CB_2 receptors expressed in CHO cells were from Perkin-Elmer Life and Analytical Sciences (U.S.). All other reagents were derived from commercial sources.

CHO cells transfected with human CB_1 and CB_2 receptors were cultured in Ham's F12 containing 10% fetal bovine serum, penicillin (100 U/mL), streptomycin (100 μg/mL), and Geneticin (G418, 0.4 mg/mL) at 37 °C in 5% CO_2/95% air.[45] Cellular membranes for binding experiments were obtained as previously described.[45] Briefly, the cells were scraped off in ice-cold hypotonic buffer (5 mM Tris–HCl, 2 mM EDTA, pH 7.4), homogenized with a Polytron, centrifuged for 10 min at 1000g, and the supernatant was further centrifuged for 30 min at 100,000g. The pellet of membranes was diluted in 50 mM Tris–HCl buffer, 0.5% BSA (pH 7.4) containing 5 mM MgCl2, 2.5 mM EDTA or 1 mM EDTA for hCB_1 or hCB_2 receptor, respectively. Competition binding experiments were carried out with [^{3}H]CP-55,940 and the examined compounds at different concentrations (1 nM to 10 μM) or WIN 55,212-2, the CB_1/CB_2 standard agonist for 90 or 60 min at 30 °C for CB_1 or CB_2 receptors, respectively. Bound and free radioactivities were separated by filtering the assay mixture through Whatman GF/C glass fiber filters using a Brandel cell harvester (Brandel Instruments, Unterföhring, Germany). The filter bound radioactivity was counted on a Perkin–Elmer 2810 TR scintillation counter (Perkin–Elmer Life and Analytical Sciences, U.S.).

5.2.2. cAMP assay for human CB_2 receptors

CHO cells transfected with human CB_2 receptors were preincubated with 0.5 mM 4-(3-butoxy-4-methoxybenzyl)-2-imidazolidinone (Ro 20-1724) as a phosphodiesterase inhibitor and the effect of the novel CB compounds tested at increasing concentrations (0.1–10 μM) or WIN 55,212-2 (0.1 μM) was studied in the presence of forskolin (10 μM) by using the fluorimetric cAMP kit (cAMP direct immunoassay kit, ab65355, abcam) according to the manufacturer's instructions.

5.2.3. Data analysis

The protein concentration was evaluated by a Bio-Rad method[46] with bovine albumin as reference standard. Inhibitory binding constants, K_i, were obtained from the IC_{50} values following the Cheng and Prusoff equation: $K_i = IC_{50}/(1 + [C]/K_D)$, where [C] is the concentration of the radioligand and K_D its dissociation constant (Cheng Prusoff).[34] A weighted nonlinear least-squares curve fitting program, LIGAND, was used for computer analysis of the inhibition experiments.[47] Schild analysis was used to calculate pK_B values of **8f**, **8h** and **8j** compounds.[48] All the data are expressed as the mean ± SEM of n = 4 independent experiments. Statistical analysis of the data was performed using ANOVA followed by Dunnett's test.

5.3. Molecular modeling studies

Compounds **8f**, **8h** and **8j** were built, parameterized (Gasteiger-Huckel method) and energy minimized within MOE using MMFF94 forcefield.[49] Docking studies were performed using the previously built ligand-based human CB_2 homology model.[38] In particular, the hCB_2 inverse agonist binding site was defined taking into account any amino acids placed at 5Å distance far from the key residue S165, as described by mutagenesis data.[50] Successively, flexible docking studies were applied using the Surflex docking module implemented in Sybyl-X1.0.[51] Surflex-Dock uses an empirically derived scoring function based on the binding affinities of X-ray protein–ligand complexes.

The Surflex-Dock scoring function is a weighted sum of non-linear functions involving van der Waals surface distances between the appropriate pairs of exposed protein and ligand atoms, including hydrophobic, polar, repulsive, entropic and solvation and crash terms represented in terms of a total score conferred to any calculated conformer.

Then, the best docking geometry (selected on the basis of the SurFlex scoring functions) was refined by ligand/protein complex energy minimization (CHARMM27) by means of the MOE software. Finally, the protein–ligand complex stability was successfully assessed using a short ~1 ps run of molecular dynamics (MD) at constant temperature, followed by an all-atom energy minimization (LowModeMD implemented in MOE software). In this way, an exhaustive conformational analysis of the ligand-receptor binding site complex was explored, as we already explained about other case studies for a preliminary evaluation of the derived docking poses.[52]

5.4. In silico evaluation of pharmacokinetic properties

The prediction of ADMET properties was performed using the Advanced Chemistry Development (ACD) Percepta platform (www.acdlabs.com).

Any ADMET descriptor was evaluated by Percepta, based on training libraries implemented in the software, which include a consistent pool of molecules whose pharmacokinetic and toxicity profiles are experimentally known.

Acknowledgement

Authors acknowledge Regione Autonoma della Sardegna for economic support (grant n. CRP-26417, LR n. 7/2007 and INNOVA.RE- POR FESR 2007-2013).

Supplementary data

Supplementary data associated with this article can be found, in the online version, at http://dx.doi.org/10.1016/j.bmc.2016.08.055.

References and notes

1. Di Marzo, V.; Bifulco, M.; De Petrocellis, L. *Nat. Rev. Drug Discov.* **2004**, *3*, 771.
2. Boyd, S. T. **2006**, *26*, 218S.
3. DiPatrizio, N. V.; Piomelli, D. *Trends Neurosci.* **2012**, *35*, 403.
4. Howlett, A. C.; Barth, F.; Bonner, T. I.; Cabral, G.; Casellas, P.; Devane, W. A.; Felder, C. C.; Herkenham, M.; Mackie, K.; Martin, B. R.; Mechoulam, R.; Pertwee, R. G. *Pharmacol. Rev.* **2002**, *54*, 161.
5. Reggio, P. H. *Curr. Med. Chem.* **2010**, *17*, 1468.
6. Gaoni, Y.; Mechoulam, R. *J. Am. Chem. Soc.* **1964**, *86*, 1646.
7. Matsuda, L. A.; Lolait, S. J.; Brownstein, M. J.; Young, A. C.; Bonner, T. I. *Nature* **1990**, *346*, 561.
8. Adams, I. B.; Martin, B. R. *Addiction* **1996**, *91*, 1585.
9. Pertwee, R. G.; Howlett, A. C.; Abood, M. E.; Alexander, S. P. H.; Di Marzo, V.; Elphick, M. R.; Greasley, P. J.; Hansen, H. S.; Kunos, G.; Mackie, K.; Mechoulam, R.; Ross, R. A. *Pharmacol. Rev.* **2010**, *62*, 588.
10. Freund, T. F.; Katona, I.; Piomelli, D. *Physiol. Rev.* **2003**, *83*, 1017.

11. Munro, S.; Thomas, K. L.; Abu-Shaar, M. *Nature* **1993**, *365*, 61.
12. Galiegue, S.; Mary, S.; Marchand, J.; Dussossoy, D.; Carriere, D.; Carayon, P.; Bouaboula, M.; Shire, D.; Le Fur, G.; Casellas, P. *Eur. J. Biochem.* **1995**, *232*, 54.
13. Schatz, A. R.; Lee, M.; Condie, R. B.; Pulaski, J. T.; Kaminski, N. E. *Toxicol. Appl. Pharmacol.* **1997**, *142*, 278.
14. Lynn, A. B.; Herkenham, M. *J. Pharmacol. Exp. Ther.* **1994**, *268*, 1612.
15. (a) Van Sickle, M. D.; Duncan, M.; Kingsley, P. J.; Mouihate, A.; Urbani, P.; Mackie, K.; Stella, N.; Makriyannis, A.; Piomelli, D.; Davison, J. S.; Marnett, L. J.; Di Marzo, V.; Pittman, Q. J.; Patel, K. D.; Sharkey, K. A. *Science* **2005**, *310*, 329; (b) Gong, J.-P.; Onaivi, E. S.; Ishiguro, H.; Liu, Q.-R.; Tagliaferro, P. A.; Brusco, A.; Uhl, G. R. *Brain Res.* **2006**, *1071*, 10; (c) Onaivi, E. S.; Ishiguro, H.; Gong, J.-P.; Patel, S.; Perchuk, A.; Meozzi, P. A.; Myers, L.; Mora, Z.; Tagliaferro, P.; Gardner, E.; Brusco, A.; Akinshola, B. E.; Liu, Q.-R.; Hope, B.; Iwasaki, S.; Arinami, T.; Teasenfitz, L.; Uhl, G. R. *Ann. N. Y. Acad. Sci.* **2006**, *1074*, 514; (d) Ellert-Miklaszlewska, A.; Grajkowska, W.; Gabrusiewicz, K.; Kaminska, B.; Konarska, L. *Brain Res.* **2007**, *1137*, 161.
16. Rajesh, M.; Mukhopadhyay, P.; Hasko, G.; Huffman, J. W.; Mackie, K.; Pacher, P. *Br. J. Pharmacol.* **2008**, *153*, 347.
17. (a) Han, S.; Thatte, J.; Buzard, D. J.; Jones, R. M. *J. Med. Chem.* **2013**, *56*, 8224; (b) Tabrizi, M. A.; Baraldi, P. G.; Borea, P. A.; Varani, K. *Chem. Rev.* **2016**, *116*, 519.
18. (a) Murineddu, G.; Asproni, B.; Pinna, G. A. *Rec. Pat. CNS Drug Discovery* **2012**, *7*, 4; (b) Murineddu, G.; Deligia, F.; Dore, A.; Pinna, G.; Asproni, B.; Pinna, G. A. *Rec. Pat. CNS Drug Discovery* **2013**, *8*, 42.
19. Malan, T. P., Jr; Ibrahim, M. M.; Lai, J.; Vanderah, T. W.; Makriyannis, A.; Porreca, F. *Curr. Opin. Pharmacol.* **2003**, *3*, 62.
20. Quartilho, A.; Mata, H. P.; Ibrahim, M. M.; Vanderah, T. W.; Porreca, F.; Makriyannis, A.; Malan, T. P., Jr *Anesthesiology* **2003**, *99*, 955.
21. Hollinshead, S. P.; Tidwell, M. W.; Palmer, J.; Guidetti, R.; Sanderson, A.; Johnson, M. P.; Chambers, M. G.; Oskins, J.; Stratford, R.; Astles, P. C. *J. Med. Chem.* **2013**, *56*, 5722.
22. (a) Arevalo-Martin, A.; Vela, J. M.; Molina-Holgado, E.; Borrell, J.; Guaza, C. *J. Neurosci.* **2003**, *23*, 2511; (b) Zajicek, J. P.; Apostu, V. I. *CNS Drugs* **2011**, *25*, 187; (c) Gijsen, H. J.-M.; De Cleyn, M. A.-J.; Surkyn, M.; Van Lommen, G. R.-E.; Verbist, B. M.-P.; Nijsen, M. J. M.-A.; Meert, T.; Van Wauwe, J.; Aerssens, J. *Bioorg. Med. Chem. Lett.* **2012**, *22*, 547; (d) Han, S.; Zhang, F.-F.; Qian, H.-Y.; Chen, L.-L.; Pu, J.-B.; Xie, X.; Chen, J.-Z. *J. Med. Chem.* **2015**, *58*, 5751.
23. (a) Aso, E.; Juvés, S.; Maldonado, R.; Ferrer, I. J. *Alzheimer Dis.* **2013**, *35*, 847; (b) Aso, E.; Ferrer, I. *Front. Pharmacol.* **2014**, *5*, 1; (c) Cao, C.; Li, Y.; Liu, H.; Bai, G.; Mayl, J.; Lin, X.; Sutherland, K.; Nabar, N.; Cai, J. J. *Alzheimer Dis.* **2014**, *42*, 973.
24. Kim, K.; Moore, D. H.; Makriyannis, A.; Abood, M. E. *Eur. J. of Pharmacol.* **2006**, *542*, 100.
25. Lunn, C. A.; Reich, E.-P.; Fine, J. S.; Lavey, B.; Kozlowski, J. A.; Hipkin, R. W.; Lundell, D. J.; Bober, L. *Br. J. Pharmacol.* **2008**, *153*, 226.
26. (a) Yang, P.; Myint, K.-Z.; Tong, Q.; Feng, R.; Cao, H.; Almehizia, A. A.; Alqarni, M. H.; Wang, L.; Bartlow, P.; Gao, Y.; Gertsch, J.; Teramachi, J.; Kurihara, N.; Roodman, G. D.; Cheng, T.; Xie, X.-Q. *J. Med. Chem.* **2012**, *55*, 9973; (b) Yang, P.; Wang, L.; Feng, R.; Almehizia, A. A.; Tong, Q.; Myint, K.-Z.; Ouyang, Q.; Alqarni, M. H.; Wang, L.; Xie, X.-Q. *J. Med. Chem.* **2013**, *56*, 2045.
27. (a) Feng, Z.; Alqarni, M. H.; Yang, P.; Tong, Q.; Chowdhury, A.; Wang, L.; Xie, X.-Q. *J. Chem. Inf. Model* **2014**, *54*, 2483; (b) Bertini, S.; Parkkari, T.; Savinainen, J. R.; Arena, C.; Saccomanni, G.; Saguto, S.; Ligresti, A.; Allarà, M.; Bruno, A.; Marinelli, L.; Di Marzo, V.; Novellino, E.; Manera, C.; Macchia, M. *Eur. J. Med. Chem.* **2015**, *90*, 526; Bertini Chicca, A.; Arena, C.; Chicca, S.; Saccomanni, G.; Gertsch, J.; Manera, C.; Macchia, M. *Eur. J. Med. Chem.* **2016**, *116*, 252; (d) Hu, J.; Feng, Z.; Ma, S.; Zhang, Y.; Tong, Q.; Alqarni, M. H.; Gou, X.; Xie, X.-Q. *J. Chem. Inf. Model* **2016**, *56*, 1152.
28. (a) Rinaldi-Carmona, M.; Barth, F.; Millan, J.; Derocq, J.-M.; Casellas, P.; Congy, C.; Oustric, D.; Sarran, M.; Bouaboula, M.; Calandra, B.; Portier, M.; Shire, D.; Brelière, J.-C.; Le Fur, G. *J. Pharmacol. Exp. Ther.* **1998**, *284*, 644; (b) Portier, M.; Rinaldi-Carmona, M.; Pecceu, F.; Combes, T.; Poinot-Chazel, C.; Calandra, B.; Barth, F.; Le Fur, G.; Casellas, P. *J. Pharmacol. Exp. Ther.* **1999**, *288*, 582.
29. Mussinu, J.-M.; Ruiu, S.; Mule, A. C.; Pau, A.; Carai, M. A. M.; Loriga, G.; Murineddu, G.; Pinna, G. A. *Bioorg. Med. Chem.* **2003**, *11*, 251.
30. (a) Chen, J.-Z.; Wang, J.; Xie, X.-Q. *J. Chem. Inf. Model* **2007**, *47*, 1626; (b) Kotsikorou, E.; Navas, F., III; Roche, M. J.; Gilliam, A. F.; Thomas, B. F.; Seltzman, H. H.; Kumar, P.; Song, Z.-H.; Hurst, D. P.; Lynch, D. L.; Reggio, P. H. *J. Med. Chem.* **2013**, *56*, 6593.
31. Pinna, G.; Curzu, M. M.; Dore, A.; Lazzari, P.; Ruiu, S.; Pau, A.; Murineddu, G.; Pinna, G. A. *Eur. J. Med. Chem.* **2014**, *85*, 747.
32. Pinna, G.; Loriga, G.; Lazzari, P.; Ruiu, S.; Falzoi, M.; Frau, S.; Pau, A.; Murineddu, G.; Asproni, B.; Pinna, G. A. *Eur. J. Med. Chem.* **2014**, *82*, 281.
33. Dore, A.; Asproni, B.; Scampuddu, A.; Pinna, G. A.; Christoffersen, C. T.; Langgård, M.; Kehler, J. *Eur. J. Med. Chem.* **2014**, *84*, 181.
34. Cheng, Y.; Prusoff, W. H. *Biochem. Pharmacol.* **1973**, *22*, 3099.
35. Tabrizi, M. A.; Baraldi, P. G.; Ruggiero, E.; Saponaro, G.; Baraldi, S.; Poli, G.; Tuccinardi, T.; Ravani, A.; Vincenzi, F.; Borea, P. A.; Varani, K. *Eur. J. Med. Chem.* **2016**, *113*, 11.
36. Bolognini, D.; Cascio, M. G.; Parolaro, D.; Pertwee, R. G. *Br. J. Pharmacol.* **2012**, *165*, 2561.
37. Kenakin, T. *FASEB J.* **2001**, *15*, 598.
38. Cichero, E.; Menozzi, G.; Guariento, S.; Fossa, P. *Med. Chem. Commun.* **2015**, *6*, 1978.
39. Montero, C.; Campillo, N. E.; Goya, P.; Páez, J. A. *Eur. J. Med. Chem.* **2005**, *40*, 75.
40. Deiana, V.; Gómez-Cañas, M.; Pazos, M. R.; Fernández-Ruiz, J.; Asproni, B.; Cichero, E.; Fossa, P.; Muñoz, E.; Deligia, F.; Murineddu, G.; García-Arencibia, M.; Pinna, G. A. *Eur. J. Med. Chem.* **2016**, *112*, 66.
41. van de Waterbeemd, H.; Gifford, E. *Nat. Rev. Drug Discov.* **2003**, *2*, 192.
42. Suchocki, J. A.; May, E. L.; Martin, T. J.; George, C.; Martin, B. R. *J. Med. Chem.* **1991**, *34*, 1003.
43. Zhao, M.; Kuang, C.; Yang, Q.; Cheng, X. *Tetrahedron Letters* **2011**, *52*, 992.
44. Verma, A. K.; Lotla, S. K. R.; Choudhary, D.; Patel, M.; Tiwari, R. K. *J. Org. Chem.* **2013**, *78*, 4386.
45. Merighi, S.; Simioni, C.; Gessi, S.; Varani, K.; Borea, P. A. *Biochem. Pharmacol.* **2010**, *79*, 471.
46. Bradford, M. M. *Anal. Biochem.* **1976**, *72*, 248.
47. Munson, P. J.; Rodbard, D. *Anal. Biochem.* **1980**, *107*, 220.
48. Gessi, S.; Varani, K.; Merighi, S.; Morelli, A.; Ferrari, D.; Leung, E.; Baraldi, P. G.; Spalluto, G.; Borea, P. A. *Br. J. Pharmacol.* **2001**, *134*, 116.
49. MOE: Chemical Computing Group Inc. Montreal. H3A 2R7 Canada. http://www.chemcomp.com].
50. Gouldson, P.; Calandra, B.; Legoux, P.; Kernéis, A.; Rinaldi-Carmona, M.; Barth, F.; Le Fur, G.; Ferrara, P.; Shire, D. *Eur. J. Pharmacol.* **2000**, *28*, 17.
51. Sybyl-X 1.0 Tripos Inc 1699 South Hanley Road. St Louis. Missouri. 63144. USA 25.
52. (a) Fossa, P.; Cichero, E. *Bioorg. Med. Chem.* **2015**, *23*, 3215; (b) Franchini, S.; Battisti, U. M.; Prandi, A.; Tait, A.; Borsari, C.; Cichero, E.; Fossa, P.; Cilia, A.; Prezzavento, O.; Ronsisvalle, S.; Aricò, G.; Parenti, C.; Brasili, L. *Eur. J. Med. Chem.* **2016**, *112*, 1.